sustainability

MDPI

Article

Monitoring Wetland Landscape Evolution Using Landsat Time-Series Data: A Case Study of the Nantong Coast, China

Minjing Wang [1,2,3,*], Yanyan Kang [2,4], Zhuyou Sun [2,3], Jun Lei [2,4] and Xiuqiang Peng [2,3]

[1] School of Geography and Ocean Science, Nanjing University, Nanjing 210023, China
[2] Observation and Research Station of East China Coastal Zone, Ministry of Natural Resources, Nanjing 210007, China
[3] Institute of Geochemical Exploration and Marine Geological Survey, East China Mineral Exploration and Development Bureau for Non-Ferrous Metals, Nanjing 210007, China
[4] College of Oceanography, Hohai University, Nanjing 210024, China
* Correspondence: njtogether@163.com; Tel.: +86-15850513600

Abstract: Coastal wetlands not only have rich biodiversity and high productivity but also provide important ecological services. The monitoring of landscape changes can provide important support for the sustainable development of coastal zones. Landsat images from 1986 to 2017 were used to interpret the types of coastal wetlands in Nantong. A single dynamic degree and multiple landscape indices were calculated to analyze the rate of change and characteristics of each wetland type. The results demonstrate the following: (1) A Nantong wetland type system was established, which was divided into three major categories and eleven subcategories. (2) In general, natural wetlands, such as thatched and *Suaeda salsa* marshes, were extremely reduced, while artificial wetlands and non-wetlands with high human activity, such as breeding ponds, farmland, and construction land, increased significantly. (3) In the past 30 years, due to the influence of environmental pressures, such as population growth, land demand, and economic development, the major influencing factors of local landscape change have shifted from natural geographical factors to human activities and economic as well as social factors. Remote sensing wetland interpretation can be very helpful in monitoring the dynamic changes in coastal wetlands and can provide scientific support for the sustainable management of coastal zones.

Keywords: coastal wetland; landscape pattern; remote sensing; Nantong coast

check for updates

Citation: Wang, M.; Kang, Y.; Sun, Z.; Lei, J.; Peng, X. Monitoring Wetland Landscape Evolution Using Landsat Time-Series Data: A Case Study of the Nantong Coast, China. *Sustainability* **2022**, *14*, 13718. https://doi.org/10.3390/su142113718

Academic Editors: Zhenglei Xie, Gaoru Zhu and Dafang Wu

Received: 15 September 2022
Accepted: 19 October 2022
Published: 22 October 2022

Publisher's Note: MDPI stays neutral with regard to jurisdictional claims in published maps and institutional affiliations.

Copyright: © 2022 by the authors. Licensee MDPI, Basel, Switzerland. This article is an open access article distributed under the terms and conditions of the Creative Commons Attribution (CC BY) license (https://creativecommons.org/licenses/by/4.0/).

1. Introduction

Coastal systems and wetlands provide an important portion of global ecosystem services [1]. Coastal wetlands are located in the staggered transition zone between terrestrial ecosystems and marine ecosystems, and have important ecological, economic, and scientific value (valued as being up to USD 194,000 ha^{-1} yr^{-1}) [2]. Coastal wetlands not only have rich biodiversity and high productivity but also provide important services that cannot be replaced by other ecosystems, such as carbon sequestration [3], environmental purification [4], climate regulation [5], flood resistance [6], and biodiversity conservation [7]. However, they are also vulnerable areas that are being rapidly lost under the dual pressures of rising sea levels and high-intensity human activity [8–10]. Previous studies have shown that 16.02% of tidal flats were lost from 1984 to 2016, mainly due to human reclamation activities [11]. Human activities have greatly changed the landscape patterns and land-use types of coastal wetlands [12,13]. The coastal wetlands in Jiangsu Province are notable in the Asian continental margin as having the most typical tidal flats developed offshore. However, with rapid economic development, terrestrial areas have notably increased, and large areas of coastal wetlands have decreased [14,15]. In order to utilize coastal wetland resources more rationally, it is necessary to explore management strategies of the sustainable utilization of coastal wetlands by tracking the history of these coastal wetlands.

Traditional field surveys have certain limitations in terms of their monitoring scope, frequency, and intensity [16]. Combining remote sensing (RS) with geographic information system (GIS) technology, coastal landforms have been effectively monitored in near real time at different spatial scales and resolutions [17–23]. Murray et al. (2019) mapped the global tidal flats during 1984–2016 using Landsat images [11]. Li and Gong (2016) monitored the dynamics of a muddy coastline with subtle variability in western Florida at annual and subpixel scales using time series Landsat data (1984–2013) [18]. Wang et al. (2020) mapped coastal wetlands in China for 2018 using time-series Landsat imagery (ETM+/OLI images) [20]. Li et al. (2018) analyzed the land-use/cover change pattern and change process of the West Bank of Lake Baikal based on three phases of Landsat remote sensing image data, in addition to the driving forces [23]. These studies have demonstrated that Landsat images, with a long record and moderate temporal (16 days) as well as spatial resolutions (15–30 m), are useful for monitoring coastal changes over large areas. The remote sensing monitoring of coastal wetlands on a global or national scale is currently a hot topic for scholars. Jia et al. (2021) produced a tidal flat map using time-series Sentinel-2 images along the entire coastal line of China, but coastal vegetation was not included in this study [24]. Keshta et al. (2022) used Landsat satellite images to access the loss of marshes in Lake Burullus, Egypt, from 1985 to 2020, without dividing marshes according to vegetation types [25]. For specific regions, existing large-scale coastal wetland maps cannot provide detailed and up-to-date information on coastal wetlands in specific regions (counties and cities). Furthermore, most of these studies only used images from a single date or mosaicked images from multiple dates, which can lead to large spatial and temporal uncertainties. Coastal areas are often affected by low-quality observations such as clouds or cloud shadows, periodic tides, and coastal vegetation phenology [26]. Therefore, detailed and updated spatial information on coastal wetlands in specific regions, including coastal vegetated and non-vegetated tidal flats, has not been fully investigated.

Visual interpretation and supervised as well as unsupervised classification algorithms are the most commonly methods used in land-use classifications and are also widely used in coastal wetland type classification [27,28]. With the development of remote sensing automatic extraction technology, machine learning algorithms (such as random forests [13,29], support vector machines [30], neural networks [31], etc.) have become a research hotspot. However, the land cover classification methods applied on Landsat images from the 1970s to date have both strengths and limitations, and the most used method is based on maximum likelihood classification [27]. Coastal wetlands are complex, and remote sensing images often have the phenomena of 'same objects with different spectrum' and 'different objects with the same spectrum.' The phenomena of misclassification and omission in machine classification are inevitable, which requires a lot of manual processing in the later stages [32]. Liu et al. (2018) adopted a support vector machine (SVM) for mapping the invasion of *S. alterniflora*, but manual post-processing was still unavoidable [30]. In addition, in the process of visual interpretation, the interpreters can use their own knowledge and experience, combined with auxiliary data such as elevation, topography, soil, and land-use for comprehensive analyses, especially in the processing of the spatial relationship of ground objects, which is superior to automatic computer interpretation [33].

In this study, we combined field survey data and used remote sensing interpretation to extract the wetland types of five periods of remote sensing images from 1986 to 2017 in Nantong, Jiangsu, China. Using the spatial analysis method of a geographic information system, the distribution range and characteristics of various wetland types was statistically used to analyze the historical evolution process of coastal wetlands. The results could provide the local government and communities with a better understanding of the coastal wetland evolution pattern to make suitable decisions on wetland conservation, restoration, and sustainable management.

2. Materials and Methods

2.1. Study Area

The Nantong coast is located in the South Yellow Sea, on the south wing of the Radial Sand Ridges (RSRs). The RSRs is distributed in the inland shelf off the coast of Jiangsu, 199.6 km long from north to south (32°00′ N–33°48′ N) and 140 km wide from east to west (120°40′ E–122°10′ E). It is composed of more than 70 sand ridges and tidal channels, roughly with the 'Tiaozini' on the shore as the hub, and spreads out in a pleated fan shape toward the sea spokes. Its ridges and troughs are interconnected, and the water depth is bounded by 0–25 m [34]. The total area is about 22,470 km^2, of which 3782 km^2 is exposed above the water surface, with a small slope of 0.2% for the mudflats and 1.5% for the tidal channels [35,36]. The sediment type is mainly silt and fine sand, with a grain size of 62.5–250 μm [37,38].

Specifically, our study area, the southern wing of the RSRs group, is mainly composed of sand ridges and tidal channels. The sand ridges mainly include Hetunsha, Taiyangsha, Lengjiasha, and Yaosha; the tide channels are Huangshayang, Lanshayang, Wangcanghong, and Xiaomiaohong (Figure 1). The tidal nature of this sea area is irregular semi-diurnal [39]. Xiaoyangkou is the area with the strongest tidal range along the coast of Jiangsu Province, and the maximum tidal range can reach 9.36 m [40]. Ocean currents include coastal currents controlled by the circulation of the Yellow Sea, flowing from NNW, NWW to SE, and the mouth of the Yangtze River to the north, flowing clockwise along the periphery of Lengjiasha, from southeast to northwest [41]. The main waves of the coastal area are southeast in summer, northwest in winter, northeast in autumn, and east in spring.

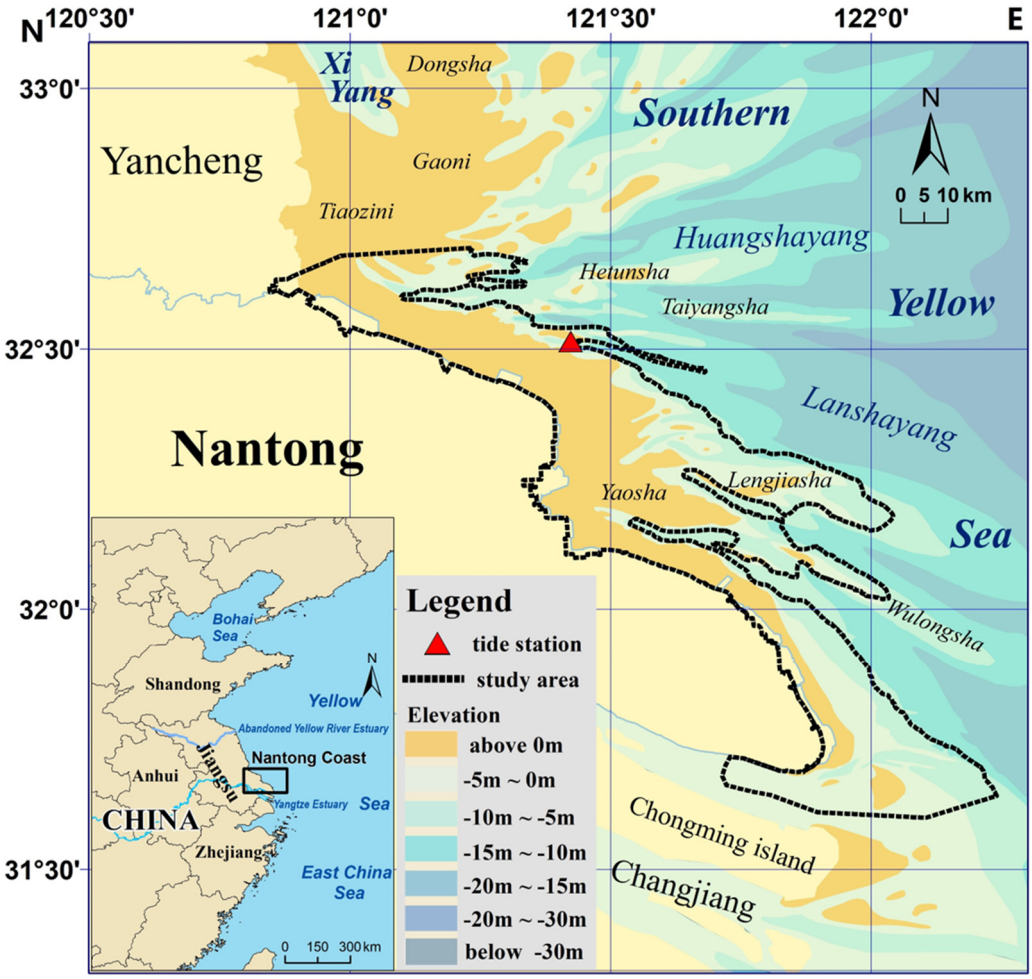

Figure 1. Location and topographic map of the Nantong coast.

The coastal wetlands in Nantong mainly include natural wetlands such as thatch, *Suaeda salsa*, *Spartina*, and bare tidal flats, as well as land-use types with a high intensity of human activities, such as farmland, breeding ponds, and construction land [42,43]. The research scope is the coastal area of Nantong. The land area was bounded by the coastline in 1980, and the sea area is about −6 m deep, shown as a black dotted line (Figure 1). This is due to the boundary of wetlands in marine water areas, which was defined in the 'Convention on Wetlands'.

2.2. Dataset

In order to investigate the spatial and temporal distribution characteristics of the Nantong coastal wetlands, we collected the satellite image data from the Landsat-5 TM, Landsat-7 ETM+, and Landsat-8 OLI images of the medium-resolution U.S. Landsat series shown in Figure 2, and recorded *Spartina*, *Suaeda salsa*, reed, agricultural land, breeding ponds, salt pans, river reservoirs, construction lands, reclamation areas, etc. in the field survey for the verification of remote sensing identification and classification. The time range of the images was from 1986 to 2017, and the details are shown in Table 1. The tide gauge data were obtained from the Yangkougang tide level station in the sea area of the RSRs (Figure 1). The historical data before 2012 were calculated by a harmonic analysis [44]. All of the remote sensing images have undergone preprocessing, such as radiometric correction and geometric correction, and the error of geometric correction was controlled within one pixel. All of the images were projected onto 'WGS_1984_UTM_Zone_51N' datum planes.

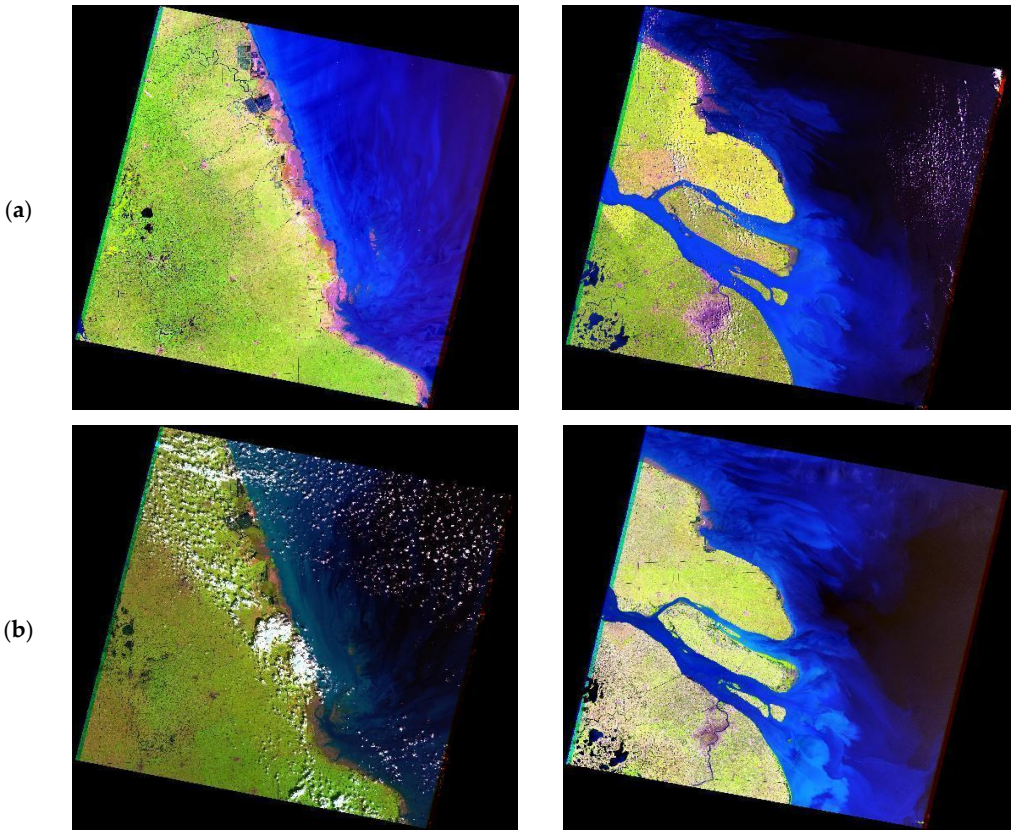

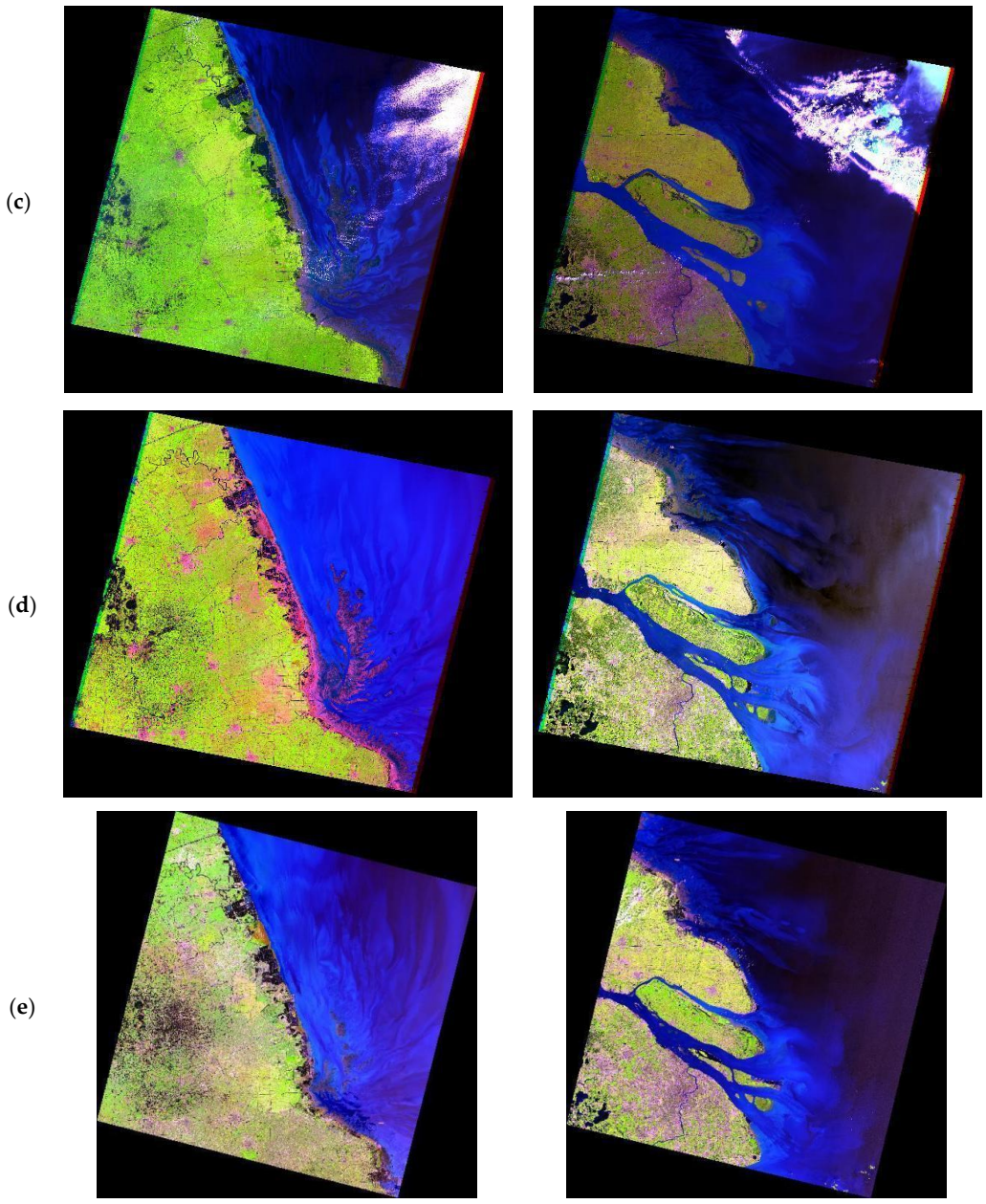

Figure 2. Landsat images covering the Nantong coast. (**a**) 1986. (**b**) 1993. (**c**) 2002. (**d**) 2008. (**e**) 2017.

Table 1. Remote sensing images and corresponding tide level data.

Date	Satellite	Sensor	WRS-2 Path/Row	Tide Level/m Yangkougang
19 August 1986	Landsat-5	TM	118/38	−2.14
22 May 1986	Landsat-5	TM	119/37	−2.40
3 June 1993	Landsat-5	TM	118/38	−2.02
30 September 1993	Landsat-5	TM	119/37	−1.92
23 August 2002	Landsat-7	ETM+	118/38	−1.85
29 July 2002	Landsat-7	ETM+	119/37	−2.10
6 July 2008	Landsat-7	ETM+	118/38	−1.97
24 April 2008	Landsat-7	ETM+	119/37	−1.82
24 August 2017	Landsat-8	OLI	118/38	−1.83
27 May 2017	Landsat-8	OLI	119/37	−1.94

2.3. Methods

2.3.1. Wetland Landscape Classification

According to the 'Convention on Wetlands,' China's wetland classification system, combined with the distribution of the Nantong coastal wetlands and the integrity of the ecosystem, a classification system of the Nantong coastal wetlands was established (Table 2) [45]. The system is generally divided into natural wetlands, artificial wetlands, and non-wetlands, including 11 categories: *Spartina* salt marsh, *Suaeda salsa* salt marsh, reed marsh, thatched marsh, bare mudflat and offshore, river bank, breeding pond, salt pan, construction land, farmland and woodland, and others (abandoned land, reclamation of unused land, etc.).

Table 2. The classification system of the coastal wetlands in Nantong.

Land Use/Landscape	Wetland	Wetland Community
Natural wetlands	Coastal wetlands	Reed marsh Thatched marsh *Suaeda salsa* salt marsh *Spartina* salt marsh Bare mudflat and offshore
	River wetland	River bank
Artificial wetland	------	Breeding pond Salt pan
Non-wetland	------	Construction land Farmland and woodland Others (abandoned land, reclamation of unused land, etc.)

2.3.2. Coastal Wetlands Interpretation

Through field surveys and remote sensing image comparisons, the coastal wetlands were interpreted to determine the interpretation signs of various landscape types and land-use types. For Swir, near-infrared, and red bands composite images of the Landsat images, the reed marshes are bright green and irregular in shape, and are mostly distributed along the supratidal zone outside the estuary; the thatched marsh area is yellow–green and irregular in shape; the vegetation of the *Suaeda salsa* is short, with dots of gray–red mixed with green spots; outside the *Suaeda salsa* is a dark green or brown *Spartina* salt marsh; and bare mudflats and offshore are gray–pink or dark gray due to differences in moisture content. Breeding ponds and salt pans are generally dark blue, and the distribution information of large-scale salt pans is clearly distinguishable from that of breeding ponds; the shape of farmland is generally regular, mostly grass green; woodland is green, but most of the coastal embankments are distributed in strips; and the construction land is generally irregular in shape, with red mottled spots.

According to the color tone, shape, texture, and spatial relationship of remote sensing images, as well as field survey photos, based on expert knowledge, the interpretation marks of Nantong coastal wetland types were determined (Table 3). A man–computer interactive method, combining supervised classification and artificial visual interpretation, was used to identify the wetland types via ENVI 5.2 software and ArcGIS 10.4 software. Two groups of training samples were established according to the marks and field observation points. One group was used for supervised classification by the method of maximum likelihood, and the other one was used to verify classification accuracy. The Kappa coefficients were all above 0.85, and the interpretation accuracy reached 90%.

Table 3. Comparison of remote sensing maps and corresponding field photos.

Wetland Community Type	Remote Sensing Image (RGB: Swir, Near-Infrared, and Red Bands)	Field Verification Photos
Reed marsh		
Thatched marsh		
Suaeda salsa salt marsh		
Spartina salt marsh		
Bare mudflat and offshore		
River bank		

Table 3. *Cont.*

Wetland Community Type	Remote Sensing Image (RGB: Swir, Near-Infrared, and Red Bands)	Field Verification Photos
Breeding pond		
Salt pan	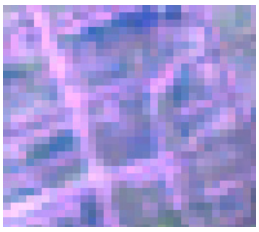	
Construction land		
Farmland and woodland	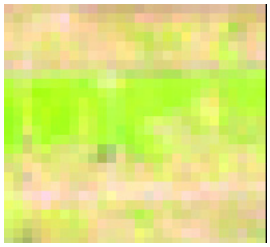	

2.3.3. Landscape Change Analysis

The most direct manifestation of landscape pattern change is land-use change. Changes in land use lead to changes in the quantity and spatial combination of land areas, which, in turn, lead to changes in landscape patterns, thus affecting the matrix and structure of landscape types in a region [46]. Two methods were used for landscape change analysis.

A single landscape dynamic model (Formula (1)) was used to analyze the degree of change in the landscape area of the study area in different time periods. This study has four time periods: 1986–1993, 1993–2002, 2002–2008, and 2008–2017.

$$K = \frac{U_b - U_a}{U_a} \times \frac{1}{T} \times 100\% \quad (1)$$

In the formula, K is the dynamic degree of a wetland landscape; U_a and U_b are a wetland area at the initial stage and the end stage, respectively; and T is the interval years.

Landscape metrics or indices have been commonly used for analyzing land-use dynamics and urban growth processes [47–49]. Landscape indices, such as the number of patches, NP; patch density, PD; largest patch index, LPI; AREA_MN; fractal dimension index, FRAC_MN; contagion index, CONTAG; Shannon's diversity index, SHDI; Shannon's evenness index, SHEI; and the aggregation index, AI, were calculated by Fragstats 4.2 software.

3. Results

3.1. Spatial Distribution of Wetland Types

The images of five periods in the coastal area of Nantong, Jiangsu were interpreted, and the classification results are shown in Figure 3. The results show that the composition of the entire Nantong coastal wetland landscape has changed significantly in the 30 years from 1986 to 2017 (Figure 4). The total area of coastal wetlands continued to decrease from 3555.25 km^2 in 1986 to 3328.55 km^2 in 2017. Among them, the natural wetland area decreased from 3551.91 km^2 in 1986 to 3179.08 km^2 in 2017. A total of 10.5% of natural wetlands have been lost over the past 30 years. The area of natural wetlands lost during 2008–2017 was significantly larger than that during 1986–1993, 1993–2002, and 2002–2008, and the loss rate of natural wetlands was also the largest. The area of artificial wetlands and non-wetland with a high intensity of human activities, such as breeding ponds, farmland, and construction land, increased significantly.

In natural wetlands, the salt marsh of *Suaeda salsa* decreased, while the salt marsh of *Spartina* increased, and the change in the reed and thatch was not obvious. Among them, the reed marsh first increased and then decreased from 17.36 km^2 in 1986, and increased again in recent years, reaching 58.59 km^2 in 2017, which was related to artificial planting and growth in the reclamation area. Thatched marsh has decreased significantly in recent years. The area of *Suaeda salsa* decreased from 77.21 km^2 in 1986 to 3.9 km^2 in 2017, with the greatest degree of degradation. In order to protect the coast and reduce coastal erosion, since the 1960s, *Spartina* has been introduced in Jiangsu, China, to promote siltation. The results in 1986 showed that the area of *Spartina* salt marshes reached 45.33 km^2 and has maintained a high growth range since then. However, due to the 1990s, the large-scale reclamation has reduced the area of *Spartina* to some extent, about 37.66 km^2 in 2002, but it still maintained growth due to its good environmental adaptability, and the area reached 59.14 km^2 in 2008. Under the background of large-scale reclamation, the area of *Spartina* salt marshes decreased, but there was still 47.11 km^2 in 2017. In a word, the main change characteristic of the Nantong coastal wetlands is that the natural wetlands represented by thatched grass and *Suaeda salsa* were greatly reduced.

Most of the artificial wetlands and farmland, such as breeding ponds and salt pans in the study area, were transformed through the reclamation and utilization of natural wetlands by humans. The area of artificial wetlands showed a trend of substantial increase. The area of breeding ponds increased from 3.34 km^2 in 1986 to 149.47 km^2 in 2017. The area of salt pans has not changed much, and there were occasional staggered distributions in the breeding pond area. By 2017, there were no salt pans, and they were all used by breeding ponds, agriculture, and industry.

In the non-wetland landscape types, farmland, woodland, and construction land continued to increase. Among them, farmland and woodland increased from 0 to 76.55 km^2 in 2017. Since 1986, construction land grew from 0 to 93.5 km^2 in 2017, a significant increase.

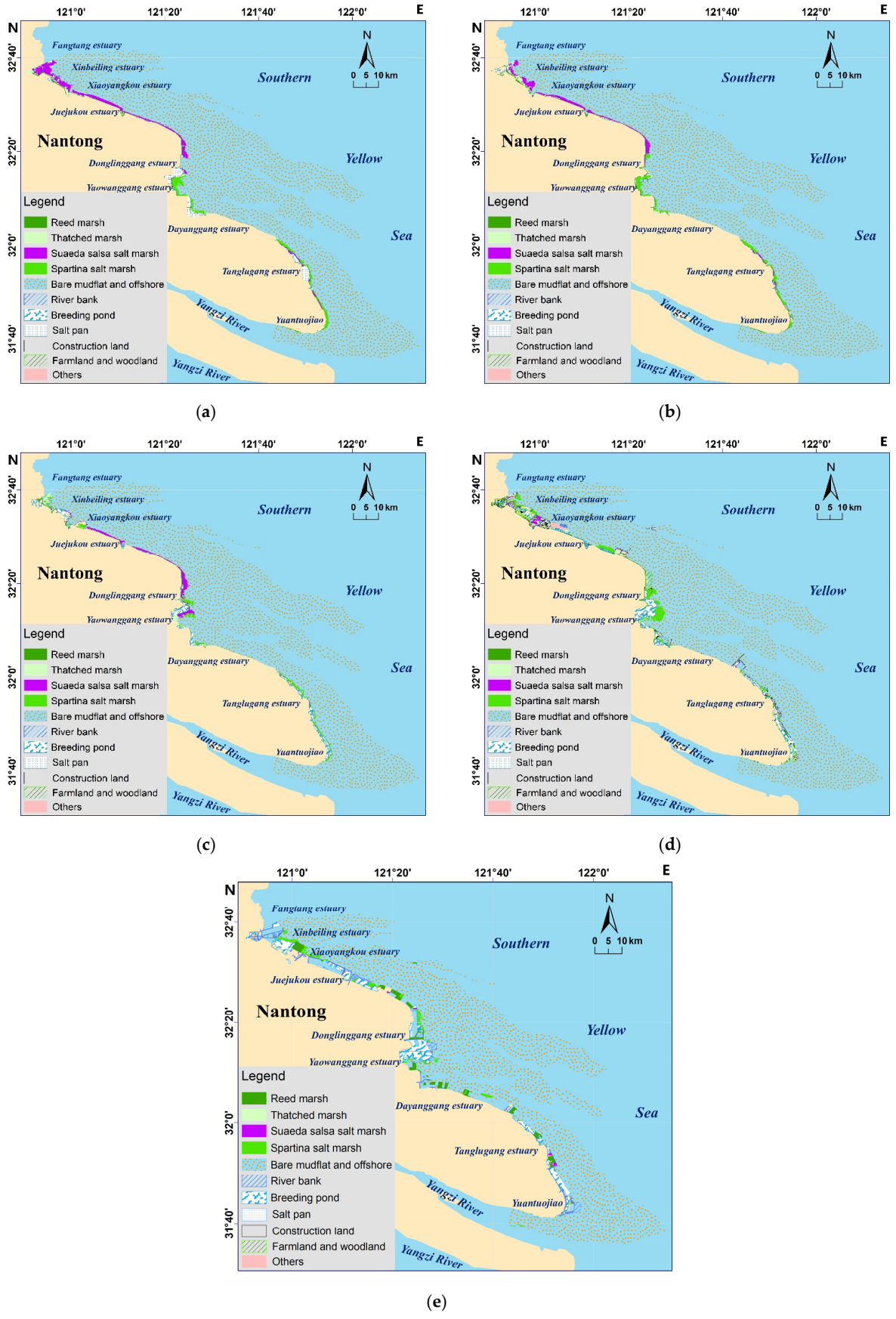

Figure 3. Distribution map of wetland types in different years. (**a**) 1986. (**b**) 1993. (**c**) 2002. (**d**) 2008. (**e**) 2017.

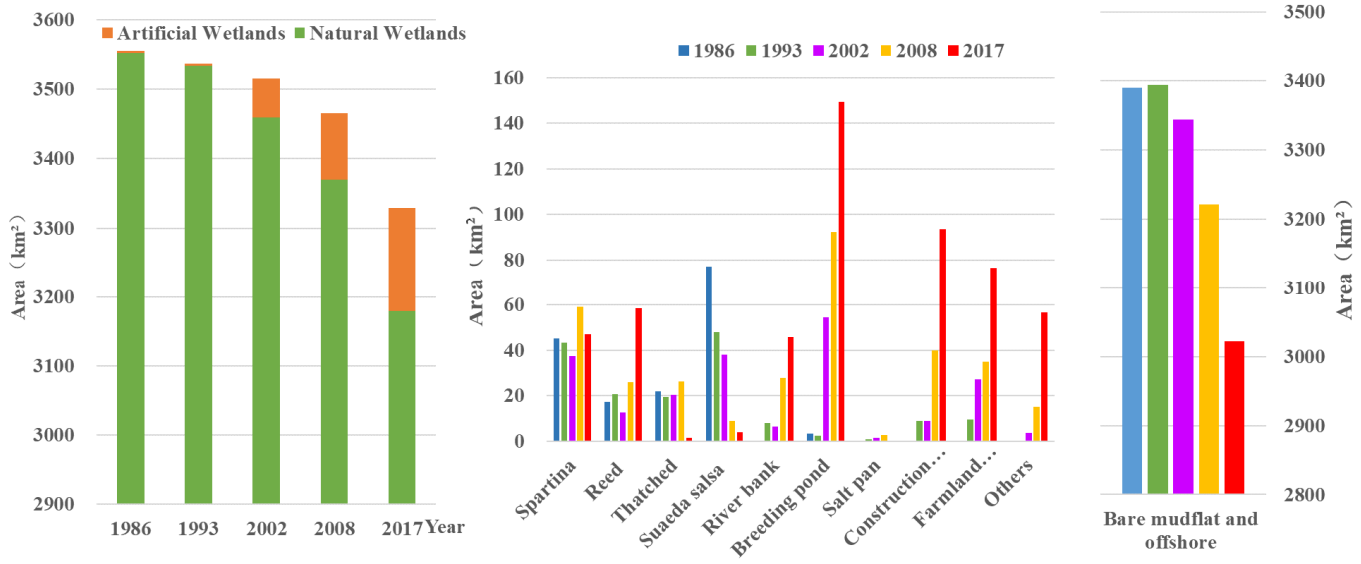

Figure 4. Landscape type area changes of the Nantong coastal wetlands in different periods. (**a**) Natural and artificial wetlands. (**b**) Different landscape types.

3.2. Change Rate and Dynamic Degree of the Nantong Coastal Wetland Types

The dynamics of each single landscape type of coastal wetlands in four time periods were statistically analyzed using Formula 1 from the Section 2. The results (Table 4) showed that during the 30 years from 1986 to 2017, the *Suaeda salsa* salt marsh had the highest dynamic degree, with an average annual change rate of −20%, especially in the period of 2002–2008, where the reduction degree reached 53.9%. The second was non-wetland types, such as construction land. The average annual change rate of construction land was 8.4%. The average annual change rate of farmland, woodland, and other landscapes was 7.9% and exceeded 10% in some periods. Artificial wetlands also had a high degree of dynamics. The average change rates of breeding ponds and salt pans were 4.1% and 6.2%, with some periods exceeding 10%.

Table 4. Dynamic degree of single landscape types of the Nantong coastal wetlands.

Wetland Type	1986–1993	1993–2002	2002–2008	2008–2017	Average
Spartina salt marsh	−0.7%	−1.8%	6.1%	−2.8%	0.2%
Reed and thatched marsh	0.4%	−2.4%	6.2%	1.4%	1.4%
Suaeda salsa salt marsh	−8.8%	−2.8%	−53.9%	−14.6%	−20.0%
Bare mudflat and offshore	0.0%	−0.2%	−0.6%	−0.7%	−0.4%
River bank	13.6%	−2.7%	12.9%	4.4%	7.0%
Breeding pond	−5.2%	10.6%	6.8%	4.2%	4.1%
Salt pan	14.3%	3.9%	6.8%	0.0%	6.2%
Construction land	14.3%	−0.1%	12.9%	6.4%	8.4%
Farmland and woodland	14.3%	7.2%	3.7%	6.0%	7.8%
Others	0.0%	11.1%	12.5%	8.1%	7.9%

3.3. Landscape Index Analysis

Number of patches and patch density: As shown in Figure 5, from 1986 to 2017, the number of patches in the bare mudflat and offshore, *Suaeda salsa*, reed, thatch, and breeding ponds increased first and then decreased. In particular, reed, thatch, and *Suaeda salsa* decreased significantly in the past decade, from 254 to 51 in total. The number of patches of river banks, *Spartina* salt marshes, and farmland showed a trend of 'increase-decrease-increase.' The amount of land for construction and other uses increased significantly, from

0 to 325 in total. The variation trend of patch density was basically consistent with the number of patches.

Mean patch area and largest patch index: As shown in Figure 6, from 1986 to 2017, the average patch area of river banks and salt pans increased first and then decreased; *Suaeda salsa*, construction land, reed, thatch, and *Spartina* salt marshes decreased first and then increased; and breeding ponds as well as farmland continued to increase, from 4.69 to 276.41 and from 0 to 107.76, respectively. The largest patch index of construction land, river bank, farmland and woodland, breeding ponds, and others showed a significant upward trend. However, the largest patch index of bare mudflat and offshore as well as *Suaeda salsa* salt marshes continued to decrease, from 95.33 to 84.98 and from 0.62 to 0.04, respectively, while other landscape types changed their volatility.

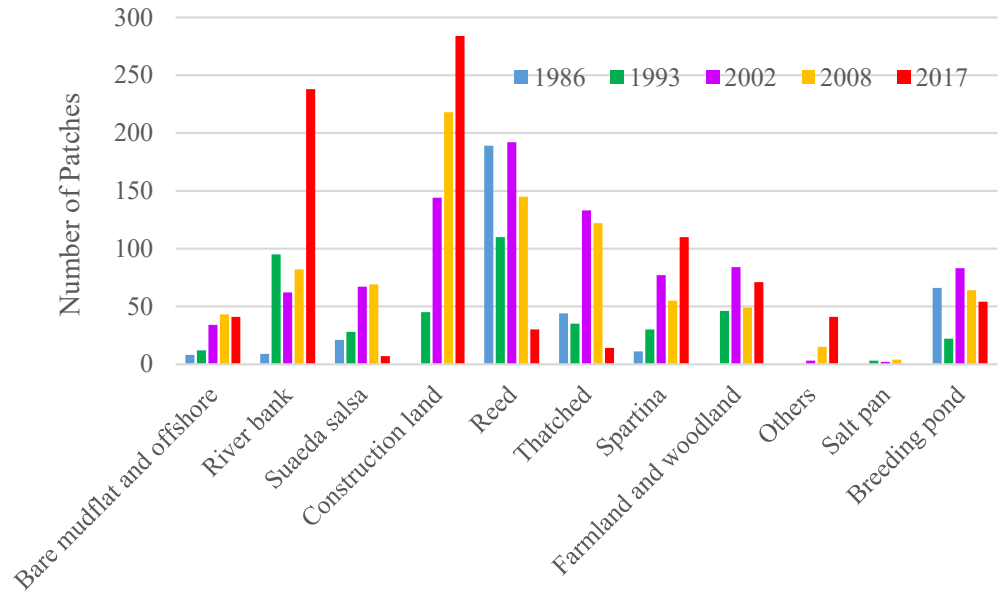

(**a**)

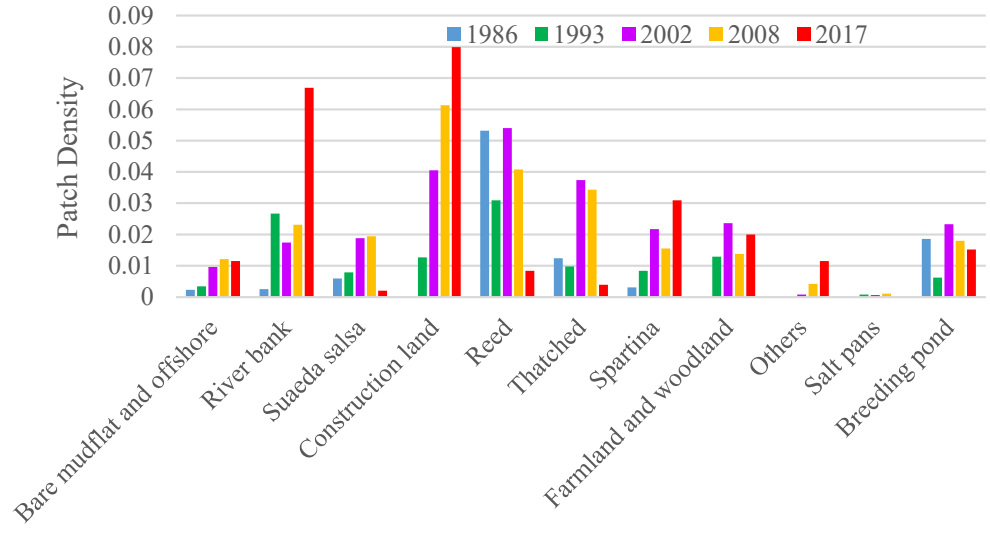

(**b**)

Figure 5. Changes in patch number and density. (**a**) Number of patches. (**b**) Patch density.

Fractal dimension index: The larger the fractal dimension of the landscape patch, the more complex the edge of the patch. As shown in Figure 7, except for bare mudflat and offshore, the average fractal dimension of other natural wetlands was higher than 1.06. The reason for this may be that *Spartina alterniflora*, *Suaeda salsa,* and reed have similar ecological niches, while *Spartina alterniflora* has a growth advantage and gradually invades other wetland communities. The average fractal dimension of artificial wetlands was higher. In general, the average fractal dimension of each landscape type over the 30 years was higher than 1.05.

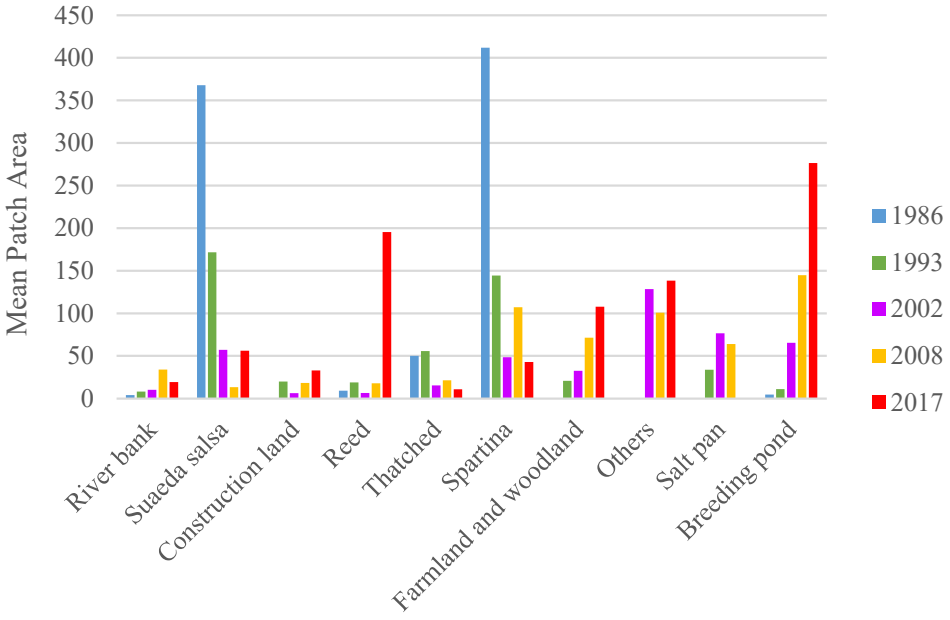

(**a**)

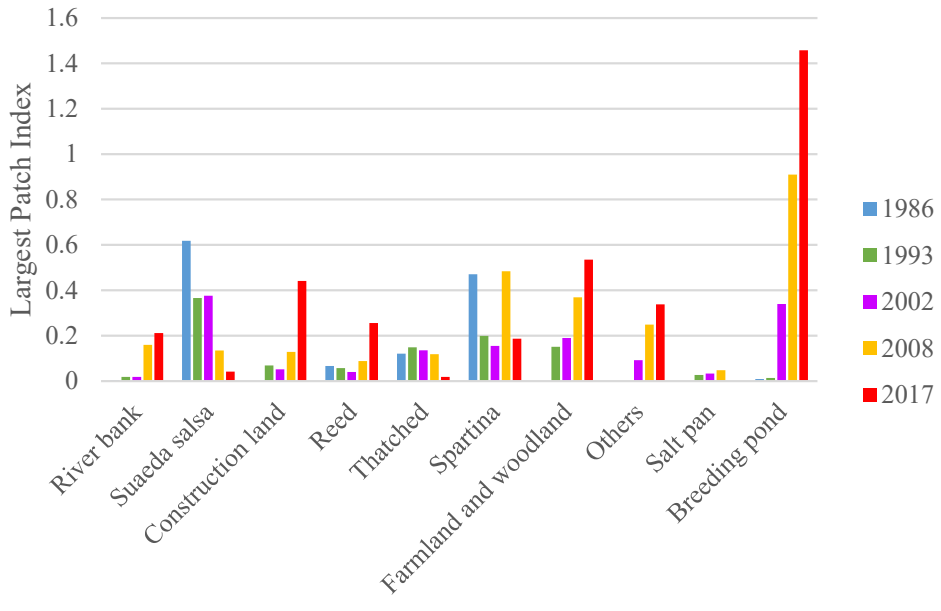

(**b**)

Figure 6. Changes in mean patch area and largest patch index. (**a**) Mean patch area. (**b**) Largest patch index.

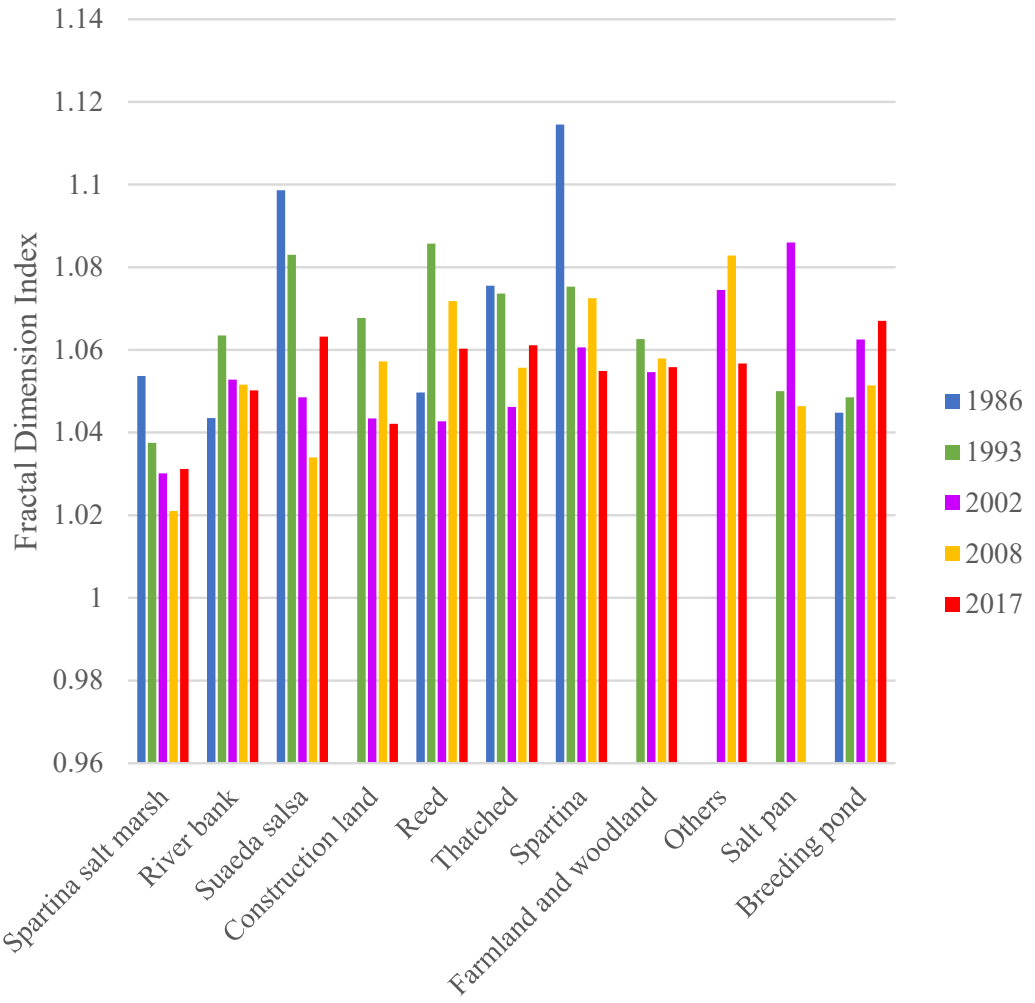

Figure 7. Average fractal dimension index distribution plot.

Shannon's diversity index and evenness index: As shown in Figure 8a,b, although the diversity changes were small from 1986 to 1993, at 0.02, the range of changes increased from 1993 to 2017, from 0.08 to 0.21, indicating that the differences in various wetland landscape types widened and that the degree of landscape heterogeneity increased. The change in the landscape diversity index better reflected the process of rapid increases in the intensity of human activities such as reclamation and port construction in the Nantong coastal zone. The change trend in the evenness index was basically the same as that of the diversity index, showing an increasing trend from 1993 to 2017, from 0.12 to 0.31. The distribution of different wetland landscape types became increasingly uniform, and the difference in proportional structure gradually decreased.

Contagion index and aggregation index: As shown in Figure 8c,d, from 1986 to 2017, the value of the contagion index fluctuated within a small range, from 0.26 to 0.30. The landscapes in the study area were relatively fragmented, with many small patches, and were mainly affected by a few large landscape types (bare mudflat and offshore, breeding ponds, etc.). The aggregation index showed a continuous decreasing trend, from 98.73 to 97.63, indicating that the aggregation degree between patches of different landscape types continued to weaken and that the fragmentation degree increased. This is consistent with the findings of the diversity index and evenness index, mainly due to the disturbance of human activities and construction.

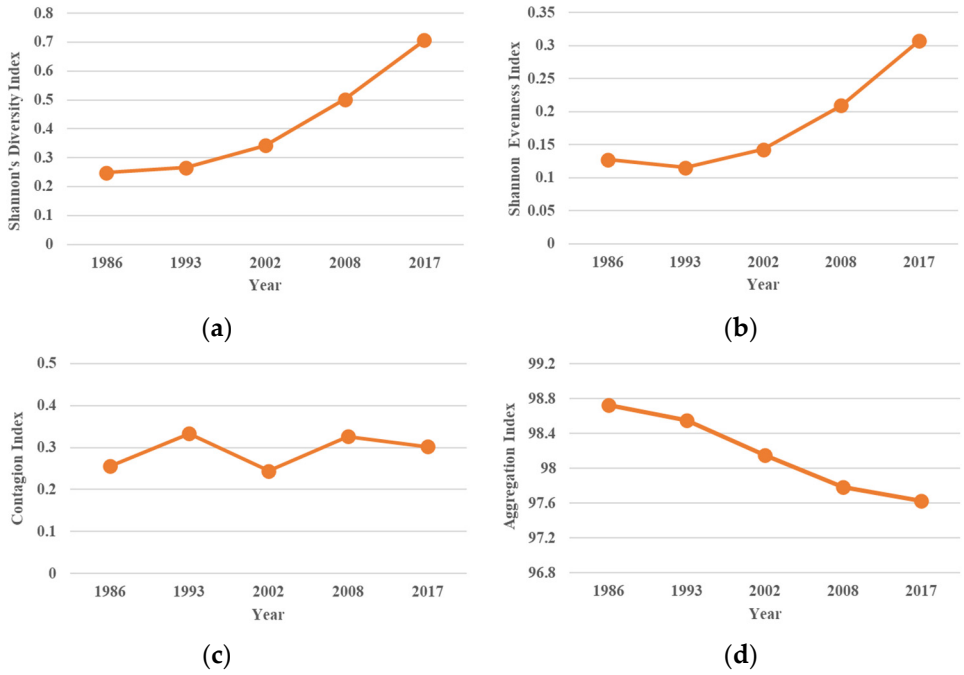

Figure 8. Variation curve of landscape indices with years. (**a**) Shannon's diversity index. (**b**) Shannon's evenness index. (**c**) Contagion index. (**d**) Aggregation index.

4. Discussion

4.1. Influence Factors

The landscape changes in the Nantong coastal wetlands are mainly controlled by three factors: one is the natural geographical conditions, the second is the demand for land, and the third is the difference in economic comparative interests. The latter two are both human interferences. In different periods, these three factors have different impacts on the changes in the Nantong coastal wetland landscape, and, in many cases, they are complementary and inseparable from each other.

4.1.1. Influence of Natural Conditions

As far as natural conditions are concerned, there were two main factors that caused the differences in the structure and pattern of the Nantong coastal wetlands landscape. On the one hand, the difference in the types of coastal erosion and deposition resulted in the difference in the abundance and shortage of reserve resources for coastal land development and utilization. This caused the north–south difference in the landscape structure, especially the landscape structure with natural covering as the main body. Nantong is dominated by long silt coasts, especially the coast north of Dayanggang. The salt marsh vegetation coverage in this area is high, and the main vegetation types grow in patches, especially in the estuary area, such as Donglinggang and Yaowanggang. From the shore to the sea, the patchy distribution of reed–thatch–*Suaeda* marshes changed from the patchy distribution of reed–thatch–*Spartina* salt marshes. On the other hand, ecological succession caused changes in the landscape pattern of coastal wetlands. The coastal ecosystem itself has a natural succession process: From the sea to the land, presenting a cross-sectional distribution of 'subtidal zone–intertidal zone (bare mudflat)–*Spartina*–*Suaeda salsa*–reed and thatch.' Corresponding to this section, the elevation of the coastal wetlands increased slightly, the soil salinity gradually decreased, and the plant types with different salt tolerances and flood tolerances grew in segments, thus forming different landscape types.

4.1.2. Impact of Reclamation

With population growth and economic development, in the late 1960s and 1970s, in order to solve the contradiction between more people and less land, the movement of

reclaiming land from the sea with the main purpose of increasing the area of arable land arose. By the 1990s, more than 140 km^2 of tidal flats had been reclaimed in the Nantong coastal zone [50]. However, due to poor development conditions and low economic benefits, the reclamation speed was not fast, and the scale was not large. In the early 1990s, Nantong actively responded to Jiangsu's strategic idea of 'Construction of Maritime Sudong' and, accordingly issued some preferential policies for the development of coastal tidal flats, such as special concessions for developers in areas with poor locations and resource conditions. As a result, the development activities of the Nantong coastal zone have also entered a new stage. On the one hand, in order to develop tidal flats, the construction of infrastructure in coastal areas has been further strengthened. On the other hand, diversified management and the development of tidal flats have been implemented, and the construction of supporting facilities for reclamation development and utilization (mainly irrigation channels, roads, etc.) has been increased. From 1993 to 2002, the area of breeding ponds increased by more than 20 times. Since 2009, a new round of tidal flat reclamation and port development as well as construction has set off a new round of climaxes. The mode of utilization has also changed significantly, from the main form of agriculture and fishery to a combination of agriculture, fishery, and industrial parks. These development patterns around the comprehensive utilization of tidal flats will inevitably affect the landscape structure and pattern of the Nantong coastal wetlands ecosystem.

In addition to reclamation, port development as well as expansion are also some of the main reasons for the loss of coastal wetlands and changes in landscape patterns. The construction of Yangkou Port, Tongzhouwan Port, and these coastal industrial parks have all become significant factors in the changing of the land use of the Nantong coastal areas in this century. The construction of ports isolates the wetlands into small habitat patches, cutting off the connection between them and interfering with the normal migration of organisms.

Finally, the human-induced invasion of alien species has a huge impact. Since 1982, Jiangsu coastal wetlands have developed into the largest *Spartina alterniflora* salt marsh ecosystem in China. The coastal area of Nantong was the earliest area where *Spartina* was introduced. The growth and spread of *Spartina alterniflora* has had a very significant impact on the landscape pattern and changes in its coastal wetlands.

4.1.3. Difference in Economic Comparative Interests

Differences in comparative interests in land use are another important cause of changes in coastal landscape patterns. The characteristic of coastal landscape change is that it evolves in the direction of maximizing land-use value because under the situation of economic diversification, people gradually realize that diversification can bring more lucrative benefits. For example, in the late 1970s, the utilization of the Nantong coastal zone was still dominated by agriculture. By the 1980s, it appeared that grain and cotton production in addition to aquaculture were the mainstays, and the comprehensive development and scale management of agriculture, forestry, animal husbandry, fishery, and salt were implemented. The utilization of tidal flats has gradually developed in a diversified direction, and the development benefits have been greatly improved. Over the years, a production and utilization pattern of the coexistence of ports, grain and cotton, shrimp, eel, freshwater fish, forest fruit, animal husbandry, clams, seaweed, and reeds has been gradually formed to maximize the comparative benefits of land. With the diversification of land use, the fragmentation of the coastal zone landscape increases, and the landscape presents a landscape change trend in multiadvantage development.

4.2. The Importance and Future of the Nantong Coast

Silty sand muddy coasts are widely distributed in China, accounting for about one-third of the coastline. Among them, the Nantong coast of Jiangsu is the most typical area. Therefore, the trend and magnitude of landscape change in the Nantong coastal area represent the changing characteristics of coastal wetlands along the silty sand muddy

coast of China. The Nantong coastal wetlands are characterized by rich biodiversity, high productivity and ecological effects, and high potential economic value. The unscientific land reclamation and coastal development activities in the past decades have led to a significant decrease in natural wetlands and a significant increase in non-wetland land-use practices. In response to this prominent problem, the National Development and Reform Commission and the Ministry of Natural Resources jointly issued the Master Plan for Major Projects for the Protection and Restoration of Nationally Important Ecosystems (2021–2035), which includes major projects for the ecological protection and restoration of coastal wetlands as a major strategy. The Nantong coast will also carry out specific projects for the protection and restoration of coastal wetlands in the future. This study will provide a scientific basis for specific coastal wetland protection and restoration projects and can provide scientific support for the preparation and implementation of the comprehensive protection and utilization plan of the coastal zone in the national coastal area.

4.3. Deficiencies and Prospect of Our Study

In this study, we used remote sensing images (five representative time points) combined with field surveys to classify landscape types, and achieved credible results, but there are still shortcomings to be improved. First, for time-series, we need to add more remote sensing images and obtain time-series results with shorter intervals, such as a 1-year interval, which will be more beneficial for us to observe more details of landscape changes. Second, in terms of remote sensing interpretation methods, the application of high-level classification methods, such as deep learning, have higher accuracy than traditional methods, such as supervised classification. In the next step, we will combine field survey data to build a database of remote sensing interpretation samples for various landscape types to support the development of reliable intelligent interpretation methods and provide a data base for subsequent landscape change analysis. Again, there is little information on the underwater topography in this study area, and the specific location of the −6 m isobath needs to be corroborated by more field measurements. Therefore, the change of underwater topography is not well considered in the area statistics. In the next step, we will expand the remote sensing interpretation method of underwater topography and revise the research scope of coastal wetlands in different periods to reduce the error.

5. Conclusions

Taking the coastal wetlands in Nantong, Jiangsu, China as the study area, combining field investigation and remote sensing interpretations, we extracted wetland types from the five-period remote sensing images from 1986 to 2017. A single dynamic model and multiple landscape indices method was used to analyze the variation characteristics of various types of coastal wetlands.

The main findings are as follows:

(1) The Nantong wetland type system was established, which was divided into three major categories: natural wetland landscapes, artificial wetland landscapes, and non-wetland landscapes, including 11 subcategories (reed marsh, thatched marsh, *Suaeda salsa* salt marsh, *Spartina* salt marsh, bare mudflat and offshore, river bank, breeding pond, salt pan, construction land, farmland and woodland, and others (abandoned land, reclamation of unused land, etc.)).

(2) Natural wetlands, such as thatched and *Suaeda salsa* marshes, were extremely reduced, while artificial wetlands and non-wetland with high human activity, such as breeding ponds, farmland, and construction land, increased significantly in the Nantong coast. The two types of natural wetland vegetation showed opposite trends as a whole in the past 30 years. The area of salt marshes of *Suaeda salsa* shrunk rapidly, while the area of salt marshes of *Spartina* increased significantly.

(3) In the past 30 years, due to the influence of environmental pressures such as population growth, land demand, and economic development, the major influencing factors of local landscape change shifted from natural geographical factors to human activities and economic as well as social factors. With the diversification of land use, the fragmentation of the coastal zone landscape increased, and the landscape presented a landscape change trend of multiadvantage development. Therefore, it is worth noting that reduced human activities and increased conservation as well as restoration efforts should be implemented to bring a stable increasing trend to the Nantong coastal wetlands.

Author Contributions: Conceptualization, M.W., Z.S. and X.P.; data curation, Y.K.; formal analysis, J.L.; investigation, Z.S. and J.L.; methodology, M.W. and X.P.; resources, Y.K.; software, M.W. and J.L.; validation, M.W. and J.L.; writing—original draft, M.W. and Y.K.; writing—review and editing, Y.K. All authors have read and agreed to the published version of the manuscript.

Funding: This research was funded by the Open Fund of Observation and Research Station of East China Coastal Zone, Ministry of Natural Resources (ORSECCZ2022101) and Jiangsu Marine Science and Technology Innovation Project (JSZRHYKJ202213).

Institutional Review Board Statement: Not applicable.

Informed Consent Statement: Not applicable.

Data Availability Statement: The data presented in this research are available upon request from the corresponding authors.

Acknowledgments: The authors appreciate the anonymous reviewers for their constructive comments and suggestions that significantly improved the quality of this manuscript. The authors are grateful to the United States Geological Survey (USGS) for providing these Landsat images. We thank Ding Xianrong and Ge Xiaoping for their valuable comments on the draft and for their support in obtaining tide level data.

Conflicts of Interest: The authors declare no conflict of interest.

References

1. Costanza, R.; d'Arge, R.; de Groot, R.; Farber, S.; Grasso, M.; Hannon, B.; Limburg, K.; Naeem, S.; O'Neill, R.V.; Paruelo, J.; et al. The value of the world's ecosystem services and natural capital. *Nature* **1997**, *387*, 253–260. [CrossRef]
2. Costanza, R.; de Groot, R.; Sutton, P.; Van der Ploeg, S.; Anderson, S.J.; Kubiszewski, I.; Farber, S.; Turner, R.K. Changes in the global value of ecosystem services. *Glob. Environ. Chang.* **2014**, *26*, 152–158. [CrossRef]
3. McLeod, E.; Chmura, G.L.; Bouillon, S.; Salm, R.; Björk, M.; Duarte, C.M.; Lovelock, C.E.; Schlesinger, W.H.; Silliman, B.R. A blueprint for blue carbon: Toward an improved understanding of the role of vegetated coastal habitats in sequestering CO_2. *Front. Ecol. Environ.* **2011**, *9*, 552–560. [CrossRef]
4. Teuchies, J.; Vandenbruwaene, W.; Carpentier, R.; Bervoets, L.; Temmerman, S.; Wang, C.; Maris, T.; Cox, T.J.S.; Braeckel, A.V.; Meire, P. Estuaries as filters: The role of tidal marshes in trace metal removal. *PLoS ONE* **2013**, *8*, e70381. [CrossRef]
5. Schuerch, M.; Spencer, T.; Temmerman, S.; Kirwan, M.L.; Wolff, C.; Lincke, D.; McOwen, C.J.; Pickering, M.D.; Reef, R.; Vafeidis, A.T.; et al. Future response of global coastal wetlands to sea-level rise. *Nature* **2018**, *561*, 231–234. [CrossRef]
6. Temmerman, S.; Meire, P.; Bouma, T.J.; Herman, P.M.J.; Ysebaert, T.; De Vriend, H.J. Ecosystem-based coastal defence in the face of global change. *Nature* **2013**, *504*, 79–83. [CrossRef]
7. Aburto-Oropeza, O.; Ezcurra, E.; Danemann, G.; Valdez, V.; Murray, J.; Sala, E. Mangroves in the Gulf of California increase fishery yields. *Proc. Natl. Acad. Sci. USA* **2008**, *105*, 10456–10459. [CrossRef]
8. Törnqvist, T.E.; Cahoon, D.R.; Morris, J.T.; Day, J.W. Coastal wetland resilience, accelerated sea-level rise, and the importance of timescale. *AGU Adv.* **2021**, *2*, e2020AV000334. [CrossRef]
9. Couvillion, B.R.; Beck, H.; Schoolmaster, D.; Fischer, M. Land area change in coastal Louisiana (1932 to 2016). *United States Geol. Surv. Sci. Investig. Map* **2017**, *3381*, 1–16. [CrossRef]
10. Wang, X.; Xiao, X.; Xu, X.; Zou, Z.; Chen, B.; Qin, Y.; Zhang, X.; Dong, J.; Liu, D.; Pan, L.; et al. Rebound in China's coastal wetlands following conservation and restoration. *Nat. Sustain.* **2021**, *4*, 1076–1083. [CrossRef]
11. Murray, N.J.; Phinn, S.R.; DeWitt, M.; Ferrari, R.; Johnston, R.; Lyons, M.B.; Clinton, N.; Thau, D.; Fuller, R.A. The global distribution and trajectory of tidal flats. *Nature* **2019**, *565*, 222–225. [CrossRef] [PubMed]
12. Kirwan, M.L.; Megonigal, J.P. Tidal wetland stability in the face of human impacts and sea-level rise. *Nature* **2013**, *504*, 53–60. [CrossRef] [PubMed]

13. Chen, C.; Feng, J.; Wang, C.; Mao, L.; Zhang, Y. Satellite-Based Monitoring of Coastal Wetlands in Yancheng, Jiangsu Province, China. *J. Mar. Sci. Eng.* **2022**, *10*, 829. [CrossRef]
14. Yao, H. Characterizing landuse changes in 1990–2010 in the coastal zone of Nantong, Jiangsu province, China. *Ocean Coast. Manag.* **2013**, *71*, 108–115. [CrossRef]
15. Cui, L.; Li, G.; Chen, Y.; Li, L. Response of Landscape Evolution to Human Disturbances in the Coastal Wetlands in Northern Jiangsu Province, China. *Remote Sens.* **2021**, *13*, 2030. [CrossRef]
16. Ghosh, S.; Mishra, D.R.; Gitelson, A.A. Long-term monitoring of biophysical characteristics of tidal wetlands in the northern Gulf of Mexico—A methodological approach using MODIS. *Remote Sens. Environ.* **2016**, *173*, 39–58. [CrossRef]
17. Cao, W.; Zhou, Y.; Li, R.; Li, X. Mapping changes in coastlines and tidal flats in developing islands using the full time series of Landsat images. *Remote Sens. Environ.* **2020**, *239*, 111665. [CrossRef]
18. Li, W.; Gong, P. Continuous monitoring of coastline dynamics in western Florida with a 30-year time series of Landsat imagery. *Remote Sens. Environ.* **2016**, *179*, 196–209. [CrossRef]
19. Wang, X.; Xiao, X.; Zou, Z.; Chen, B.; Ma, J.; Dong, J.; Doughty, R.B.; Zhong, Q.; Qin, Y.; Dai, S.; et al. Tracking annual changes of coastal tidal flats in China during 1986–2016 through analyses of Landsat images with Google Earth Engine. *Remote Sens. Environ.* **2020**, *238*, 110987. [CrossRef]
20. Wang, X.; Xiao, X.; Zou, Z.; Hou, L.; Qin, Y.; Dong, J.; Doughty, R.B.; Chen, B.; Zhang, X.; Chen, Y.; et al. Mapping coastal wetlands of China using time series Landsat images in 2018 and Google Earth Engine. *ISPRS J. Photogramm. Remote Sens.* **2020**, *163*, 312–326. [CrossRef]
21. Bagot, P.; Huybrechts, N.; Sergent, P. Satellite-Derived Topography and Morphological Evolution around Authie Macrotidal Estuary (France). *J. Mar. Sci. Eng.* **2021**, *9*, 1354. [CrossRef]
22. Kanwal, S.; Ding, X.; Sajjad, M.; Nazeer, M.; Zia, I. Remote Sensing of Narrowing Barrier Islands along the Coast of Pakistan over Past 30 Years. *J. Mar. Sci. Eng.* **2021**, *9*, 295. [CrossRef]
23. Li, Z.; Ren, Y.; Li, J.; Li, Y.; Rykov, P.; Chen, F.; Zhang, W. Land-Use/Cover Change and Driving Mechanism on the West Bank of Lake Baikal from 2005 to 2015—A Case Study of Irkutsk City. *Sustainability* **2018**, *10*, 2904. [CrossRef]
24. Jia, M.; Wang, Z.; Mao, D.; Ren, C.; Wang, C.; Wang, Y. Rapid, robust, and automated mapping of tidal flats in China using time series Sentinel-2 images and Google Earth Engine. *Remote Sens. Environ.* **2021**, *255*, 112285. [CrossRef]
25. Keshta, A.E.; Riter, J.C.A.; Shaltout, K.H.; Baldwin, A.H.; Kearney, M.; Sharaf El-Din, A.; Eid, E.M. Loss of Coastal Wetlands in Lake Burullus, Egypt: A GIS and Remote-Sensing Study. *Sustainability* **2022**, *14*, 4980. [CrossRef]
26. Sun, C.; Liu, Y.; Zhao, S.; Zhou, M.; Yang, Y.; Li, F. Classification mapping and species identification of salt marshes based on a short-time interval NDVI time-series from HJ-1 optical imagery. *Int. J. Appl. Earth Obs. Geoinf.* **2016**, *45*, 27–41. [CrossRef]
27. Phiri, D.; Morgenroth, J. Developments in Landsat Land Cover Classification Methods: A Review. *Remote Sens.* **2017**, *9*, 967. [CrossRef]
28. Davranche, A.; Lefebvre, G.; Poulin, B. Wetland monitoring using classification trees and SPOT-5 seasonal time series. *Remote Sens. Environ.* **2010**, *114*, 552–562. [CrossRef]
29. Mahdianpari, M.; Salehi, B.; Mohammadimanesh, F.; Motagh, M. Random forest wetland classification using ALOS-2 L-band, RADARSAT-2 C-band, and TerraSAR-X imagery. *ISPRS J. Photogramm. Remote Sens.* **2017**, *130*, 13–31. [CrossRef]
30. Liu, M.; Mao, D.; Wang, Z.; Li, L.; Man, W.; Jia, M.; Ren, C.; Zhang, Y. Rapid Invasion of *Spartina alterniflora* in the Coastal Zone of Mainland China: New Observations from Landsat OLI Images. *Remote Sens.* **2018**, *10*, 1933. [CrossRef]
31. Chen, C.; Ma, Y.; Ren, G.; Wang, J. Aboveground biomass of salt-marsh vegetation in coastal wetlands: Sample expanion of in situ hyperspectral and Sentinel-2 data using a generative adversarial network. *Remote Sens. Environ.* **2022**, *270*, 112885. [CrossRef]
32. Wiberg, P.L.; Fagherazzi, S.; Kirwan, M.L. Improving predictions of salt marsh evolution through better integration of data and models. *Annu. Rev. Mar. Sci.* **2020**, *12*, 389–413. [CrossRef] [PubMed]
33. Pavlovic, V.I.; Sharma, R.; Huang, T.S. Visual interpretation of hand gestures for human-computer interaction: A review. *IEEE Trans. Pattern Anal. Mach. Intell.* **1997**, *19*, 677–695. [CrossRef]
34. Ren, M. *Comprehensive Investigation of Coastal Zone and Tidal Flat Resources, Jiangsu Province*; Ocean Press: Beijing, China, 1986; pp. 122–134. (In Chinese)
35. Wang, Y.; Zhu, D.; You, K.; Pan, S.; Zhu, X.; Zou, X.; Zhang, Y. Evolution of radiative sand ridge field of the South Yellow Sea and its sedimentary characteristics. *Sci. China Ser. D* **1999**, *42*, 97–112. [CrossRef]
36. Liu, Y.X.; Li, M.C.; Zhou, M.X.; Kang, Y.; Mao, L. Quantitative Analysis of the Waterline Method for Topographical Mapping of Tidal Flats: A Case Study in the Dongsha Sandbank, China. *Remote Sens.* **2013**, *5*, 6138–6158. [CrossRef]
37. Yao, P.; Su, M.; Wang, Z.; Rijn, L.C.V.; Zhang, C.; Chen, Y.; Stive, M.J.F. Experiment inspired numerical modeling of sediment concentration over sand–silt mixtures. *Coast. Eng.* **2015**, *105*, 75–89. [CrossRef]
38. Liu, T.; Shi, X.; Li, C.; Yang, G. The reverse sediment transport trend between abandoned Huanghe River (Yellow River) Delta and radial sand ridges along Jiangsu coastline of China—An evidence from grain size analysis. *Acta Oceanol. Sin.* **2012**, *31*, 83–91. [CrossRef]
39. Zhang, C.; Zhang, D.; Zhang, J.; Wang, Z. Tidal current-induced formation-storm-induced change-tidal current-induced recovery-Interpretation of depositional dynamics of formation and evolution of radial sand ridges on the Yellow Sea seafloor. *Sci. China (Ser. D Earth Sci.)* **1999**, *42*, 1–12. [CrossRef]

40. Kang, Y.; Ding, X.; Xu, F.; Zhang, C.; Ge, X. Topographic mapping on large-scale tidal flats with an iterative approach on the waterline method. *Estuar. Coast. Shelf Sci.* **2017**, *190*, 11–22. [CrossRef]
41. Chen, K.F.; Wang, Y.H.; Lu, P.D.; Zheng, J.H. Effects of Coastline Changes on Tide System of Yellow Sea off Jiangsu Coast, China. *China Ocean Eng.* **2009**, *23*, 741–750.
42. The 908 Special Office in Jiangsu Province. *General Report of a Marine Comprehensive Survey and Evaluation of Jiangsu*; Science Press: Beijing, China, 2012; pp. 550–612. (In Chinese)
43. Zhang, M.; Pu, L. The changing process of coastal wetlands and the effects of reclamation in Jiangsu Province in recent 30 years. *Wetl. Sci. Manag.* **2017**, *13*, 56–60. (In Chinese) [CrossRef]
44. Kang, Y.; He, J.; Wang, B.; Lei, J.; Wang, Z.; Ding, X. Geomorphic Evolution of Radial Sand Ridges in the South Yellow Sea Observed from Satellites. *Remote Sens.* **2022**, *14*, 287. [CrossRef]
45. Committee on Characterization of Wetlands; Water Science and Technology Board; Board on Environmental Studies and Toxicology; Commission on Geosciences, Environment, and Resources; National Research Council. *Wetlands: Characteristics and Boundaries*; National Academy Press: Washington, DC, USA, 1995; pp. 124–125.
46. Rogan, J.; Chen, D. Remote sensing technology for mapping and monitoring land-cover and land-use change. *Prog. Plan.* **2004**, *61*, 301–325. [CrossRef]
47. O'Neill, R.V.; Krummel, J.R.; Gardner, R.H.; Sugihara, G.; Jackson, B.; De Angelis, D.L.; Milne, B.T.; Turner, M.G.; Zygmunt, B.; Christensen, S.W.; et al. Indices of landscape pattern. *Landsc. Ecol.* **1988**, *1*, 153–162. [CrossRef]
48. Alberti, M.; Waddell, P. An integrated urban development and ecological simulation model. *Integr. Assess.* **2000**, *1*, 215–227. [CrossRef]
49. Liu, X.; Li, X.; Chen, Y.; Tan, Z.; Li, S.; Ai, B. A new landscape index for quantifying urban expanion using multi-temporal remotely sensed data. *Landsc. Ecol.* **2010**, *25*, 671–682. [CrossRef]
50. Historical Records of Nantong. Available online: http://www.ntszw.gov.cn/?c=index&a=show&id=1900 (accessed on 11 September 2022). (In Chinese)